Microstructure of the CTAB–Butanol–Octane–Water Microemulsion System: Effect of Dissolved Salts

Pushan Ayyub,*† Amarnath Maitra‡ and Dinesh O. Shah
Center for Surface Science and Engineering, Department of Chemical Engineering, University of Florida, Gainesville, FL 32611, USA

We present a microstructural study of a new water-in-oil microemulsion composed of cetyltrimethylammonium bromide (CTAB), butanol, octane and an aqueous phase. The system solubilizes relatively large proportions of metal salt solutions such as $Y(NO_3)_3$ and $Cu(NO_3)_2$. The properties studied include electrical conductivity, viscosity and effective hydrodynamic diameter (from dynamic light scattering). The non-monotonic dependence of the hydrodynamic diameter on the aqueous phase fraction has been explained by a simple equipartition model with variable surfactant aggregation number. The presence of Cu^{2+} ions in very small water-in-oil droplets (<5 nm) is found to lead to the formation of a $[CuBr_3]^-$ complex, but the complex is destroyed with an increase in the size of the droplets.

We define a microemulsion as a thermodynamically stable, optically isotropic dispersion of aqueous and hydrocarbon phases, stabilized by the presence of a surfactant. The surfactant molecule has a hydrophilic head group and lypophilic tail. It optimizes its interactions by residing at the oil/water interface and reducing the interfacial tension typically by factors of 10^{-4}–10^{-5}. In some cases, microemulsions can be regarded as nearly monodisperse droplets of water in oil (W/O) or oil in water (O/W). The coherence length of the dispersed phase is characteristically *ca.* 10 nm. An interesting feature of some W/O microemulsions is their continuous evolution into O/W microemulsions (while remaining isotropic, single phase throughout) on dilution with water. Scriven[1] and others have suggested that such an inversion may occur through the intermediate formation of a bicontinuous structure in which a continuous surfactant layer partitions the system into interpenetrating but individually continuous subvolumes of water and oil. It is therefore interesting to study the evolution of the microstructure of a microemulsion with dilution.

In recent years, microemulsions have been studied extensively because of their unique physicochemical properties and wide range of applications.[2–4] Attempts have been made to understand the nature of the fluid microstructure of a microemulsion by techniques such as NMR,[5] neutron scattering,[6] static and dynamic light scattering,[7,8] vibrational spectroscopy,[9] freeze-fracture microscopy and measurements of bulk properties such as conductivity, viscosity and dielectric relaxation.

The cationic surfactant cetyltrimethylammonium bromide (CTAB) is known to promote the formation of W/O microemulsions over comparitively wide ranges of aqueous phase content. CTAB-based microemulsions have been investigated by several authors (ref. 10, and references therein). Here we report a study of the microstructure of a new W/O microemulsion composed of CTAB (surfactant), butan-1-ol (co-surfactant), *n*-octane (hydrocarbon phase) and an aqueous phase. In particular, we study some effects of incorporating metal salts (yttrium nitrate and copper nitrate) into the aqueous phase.

Experimental

Phase diagrams were established by a progressive dilution method explained below. The ratio of the surfactant (CTAB) to the co-surfactant (butan-1-ol) was kept constant at 1:0.73 (w/w) for all measurements. A combination of the two was then treated as a single (pseudo-) component in the ternary phase diagram. We started with (typically) 20 compositions corresponding to equi-spaced points on the axis connecting the oil and surfactant vertices. Water (or a given salt solution) was added in steps to each composition and the resulting phase(s) studied after allowing sufficient time (typically 12 h) for attainment of equilibrium at 25 °C. The entire phase diagram (except the extremely surfactant-rich region) was mapped in this manner.

Electrical conductivity measurements were made at 60 Hz with a YSI Model 31 conductivity bridge. Viscosity was measured by a Brookfield Model LVTC/P rotation type viscometer. Optical absorption was studied by a Perkin Elmer Model 576 UV–VIS spectrophotometer.

Dynamic (quasi-elastic) light scattering (QELS) measurements were performed using a Spectra-Physics Series-2000 Ar^+ laser (5W) as source. The sample tube was kept in the temperature-controlled chamber of a Brookhaven Instruments BI-200SM goniometer. Scattered light at 90° was focused onto the entrance slit of an EMI-9865 photomultiplier. The time dependence of the intensity auto-correlation function of the scattered light, $C(\tau) = \langle I(0)I(\tau)\rangle$, was obtained from a 64-channel digital photon correlator (Brookhaven BI-2030). The translational diffusion coefficient (σ_T) of the droplets of the dispersed phase within the continuous phase was obtained from a non-linear least-squares fit of the correlation curve using the decay equation:

$$C(\tau) = \langle I\rangle^2[1 + b\exp(-2\Gamma\tau)] \quad (1)$$

with $\Gamma = \sigma_T q^2$. Here b and q are known experimental constants and $\langle I\rangle^2$ is the $\tau \to \infty$ value of the correlation function. The hydrodynamic equivalent spherical diameter of the microemulsion droplets is finally obtained from the Stokes–Einstein relation: $D_h = kT/3\pi\eta\sigma_T$. In each case, the samples were directly filtered into specially cleaned cylindrical cells using 0.2 μm PTFE filters.

CTAB (99%) was obtained from Sigma Chemical Co. Butan-1-ol (99.8%) and *n*-octane (Reagent grade) were obtained from Fisher Scientific Co. $Y(NO_3)_3 \cdot 5H_2O$ (99.9%) and $Cu(NO_3)_2 \cdot 2.5H_2O$ (98% ACS reagent) were from

† Present address: Materials Research Group, Tata Institute of Fundamental Research, Homi Bhabha Road, Bombay 400 005, India.

‡ Present address: Department of Chemistry, University of Delhi, Delhi 110 007, India.

Aldrich Chemical Co. Water was de-ionized and distilled before use.

Results and Discussion

Phase Diagrams

Fig. 1 shows the pseudo-ternary phase diagram (in wt.%) for the (CTAB + butanol)–octane–water system. The CTAB: butanol ratio (w/w) was held constant at 1:0.73 because this particular combination was found to maximize the solubilization of certain aqueous electrolytic phases as microemulsion. The boundaries of the homogeneous, one-phase regions are shown in the phase diagram. The water-in-oil microemulsion phase (denoted by L_2) is comparatively narrow and well separated from the oil-in-water microemulsion region, L_1. Note, however, the sharp extension of the L_1 phase to the octane-rich region. The shaded region between L_1 and L_2 represents a homogeneous, viscous, optically birefringent phase. The hatched area at the bottom of the diagram represents a thick, opaque, white gel phase. The unmarked areas in the phase diagram stand for two or three phases in co-existence.

The presence of dissolved electrolytes affects the phase diagram markedly. An increase in the concentration of $Y(NO_3)_3$ in the aqueous phase leads to an expansion in the L_2 phase and a contraction in the optically anisotropic phase. For $[Y(NO_3)_3] = 0.1$ mol dm^{-3}, the L_2 and L_1 regions merge into each other (Fig. 2). In other words, an increase in the aqueous content produces a continuous inversion of the W/O microemulsion to an O/W microemulsion within the isotropic single-phase domain.

Electrical Conductivity and Viscosity

In a microemulsion, macroscopic transport properties such as viscosity and conductivity are controlled by the microstructure. While the bulk viscosity reflects the magnitude of the inter-droplet interactions,[11] electrical conductivity depends on the local (micro-) viscosity experienced by the charge carriers.[12] For a random system of conducting spheres (aqueous droplets) in an insulating medium (oil), a rapid increase in the conductivity as a function of the droplet volume fraction indicates the first appearance of a macroscopic chain of droplets. Lang *et al.*[10] have shown that the value of this percolation threshold is related to the magnitude of the interdroplet exchange rate constant.

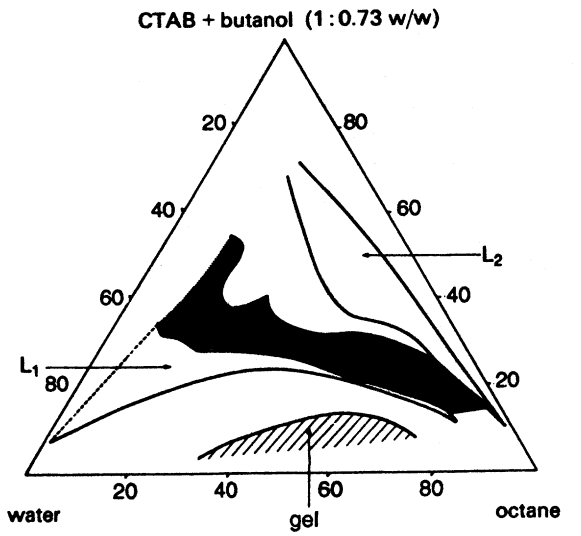

Fig. 1 Phase diagram (in wt.%) of the (CTAB + butanol)–octane–water system at 25 °C

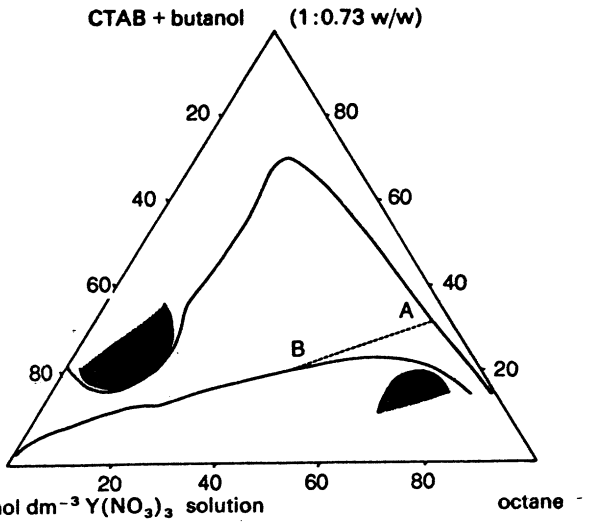

Fig. 2 Phase diagram (in wt.%) of the (CTAB + butanol)–octane–$Y(NO_3)_3$ (0.1 mol dm^{-3} solution) system at 25 °C.

Fig. 3 shows the conductivity of the (CTAB + butanol)–octane–aqueous $Y(NO_3)_3$ system at 25 °C as a function of the weight fraction of the aqueous phase. We show data for two different $Y(NO_3)_3$ concentrations and water as a limiting case. Dilution with the aqueous component in this study corresponds to a movement from A to B in the phase diagram (Fig. 2). The 'knee' in the conductivity at $f(w) \approx 12\%$, following the sharp initial rise, may be interpreted as the percolation threshold, f_p. The rather low value observed for 'f_p' could then be ascribed to clustering of droplets due to attractive interactions and a short-range hopping of the conducting species between neighbouring droplets.[13] The value of 'f_p' increases slightly with increasing salt concentration, *i.e.* with increasing number of charge carriers.

Alternatively, since percolation phenomena are often associated with steeper variations in conductivity than we observed, the 'knee' in Fig. 3 may indicate the phase inversion point between an oil-continuous and a water-continuous structure. Note that the conductivity curves are not completely flat in the 'plateau' above $f(w) \approx 12\%$. Also, the conductivity in this region is almost an order of magnitude less than that of aqueous $Y(NO_3)_3$ of the same concentration. [*E.g.*, $\log \sigma = -2.29$ for the microemulsion containing 0.4 mol dm^{-3} $Y(NO_3)_3$ with $f(w) = 30\%$, whereas $\log \sigma = -1.41$ for 0.4 mol dm^{-3} $Y(NO_3)_3$.] This appears to indicate that the microemulsion is not perfectly water-continuous just above $f(w) \approx 12\%$. The discontinuous change in the gradient

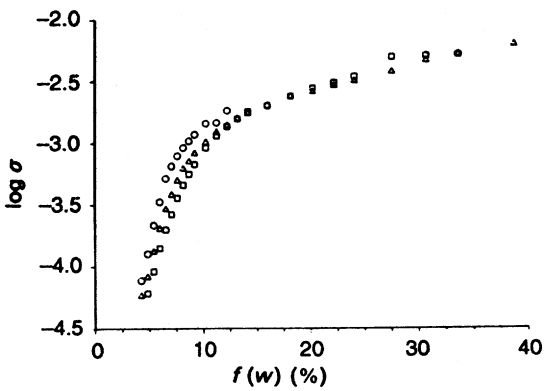

Fig. 3 Variation of the electrical conductivity (in S cm^{-1}) with aqueous fraction (wt.%) for the (CTAB + butanol)–octane–$Y(NO_3)_3$ system at 25 °C at (□) 0.4 and (△) 0.2 mol dm^{-3} of $Y(NO_3)_3$ and for (○) water

of the curve could then be ascribed to a change in the mechanism of conduction at that point.[13] Transport is dominated by the motion of droplets in the low concentration region, and by the motion of charge carriers within the neighbouring droplets of a cluster in the higher concentration region.

The viscosity behaviour of (CTAB + butanol)–octane–0.1 mol dm^{-3} $Y(NO_3)_3$ at 25 °C is shown in Fig. 4. The viscosity increases steadily below the percolation threshold, but for $f(w) > 18\%$, it becomes independent of the aqueous fraction and is much higher than that of pure octane (0.55 cP). The initial rise in the viscosity reflects an increase in interdroplet interactions.

Photon Correlation Spectroscopy

Effect of Dilution with Water

The effective hydrodynamic diameter, D_h, of the microemulsion droplets was obtained from photon correlation spectroscopy (quasi-elastic light scattering; QELS) using the technique described in the Experimental section. The effective droplet diameter for the (CTAB + butanol)–octane–aqueous $Y(NO_3)_3$ system as a function of the volume of the aqueous phase,† $V(w)$, is shown in Fig. 5. The $Y(NO_3)_3$ concentration was 0.1 mol dm^{-3}. The variation in $V(w)$ during this experiment again corresponds to a movement from A towards B in the phase diagram (Fig. 2). The system remains transparent, isotropic, single phase at all stages. In order to discuss the non-monotonic dependence of D_h on $V(w)$, it is useful to partition the curve into three regions: $0 \leq V(w) \leq 0.8$ (linear increase), $0.8 < V(w) < 1.6$ (monotonic decrease) and $1.6 \leq V(w) \leq 2.4$ (linear increase). We point out that our conductivity and viscosity data do not indicate a phase transition in the range $0.8 \leq V(w) \leq 2.4$; thus we need to look elsewhere for an explanation of the non-monotonic behaviour of D_h.

A relation between D_h and $V(w)$ can be derived from simple geometric considerations provided we accept the droplet model. The universal applicability of an 'effective diameter' obtained from QELS measurements has been questioned.[14] However, the 'simple' droplet model is generally believed to be realistic for CTAB systems with comparatively low aqueous fraction.[10] We assume that the aqueous phase is

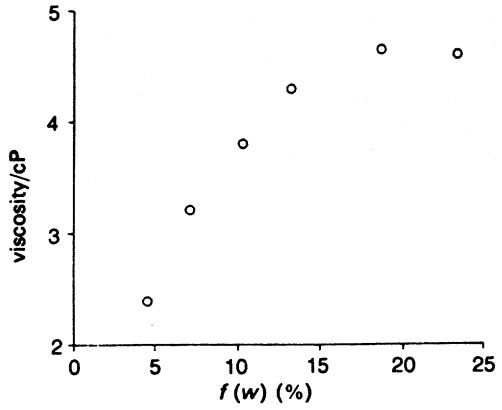

Fig. 4 Variation of the viscosity with aqueous fraction (wt.%) for the (CTAB + butanol)–octane–0.1 mol dm^{-3} $Y(NO_3)_3$ system at 25 °C

† We avoid the more commonly used parameter, $w_0 \equiv n_w/n_s$, the molar ratio of water to surfactant. We believe that in the present case the number of surfactant molecules residing at the interface is itself a function of n_w: hence the use of w_0 as an independent parameter would be misleading.

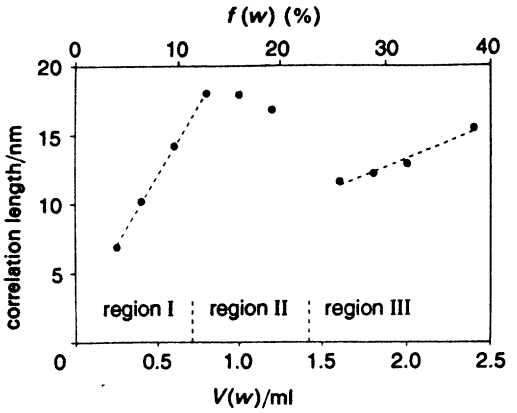

Fig. 5 Variation of the aqueous phase correlation length (measured at 25 °C) with $V(w)$. $V(w)$ is the volume (in ml) of 0.1 mol dm^{-3} $Y(NO_3)_3$ (aqueous phase) added to 1.0 g CTAB + 0.9 ml butanol + 5.0 ml octane. Data in regions I and III have been fitted with straight lines.

equipartitioned into stable, monodisperse, spherical droplets of radius ξ, each surrounded by a mono-molecular surfactant layer. Clearly:

$$\frac{\text{total water/surfactant interface area}}{\text{total volume of aqueous phase}} = \frac{3}{\xi} \qquad (2)$$

If the number of surfactant molecules at the interface is n_s, the effective cross-sectional area of the surfactant head-group is a_s and the effective length of the surfactant molecule is L_s, then:

$$D_h = 2(\xi + L_s) = \frac{6 \times 10^{21}}{n_s a_s} V(w) + 2L_s \qquad (3)$$

where $V(w)$ is in ml, a_s in nm^2; D_h, L_s and ξ are in nm.

In region I (Fig. 5), D_h follows eqn. (3) with $L_s = 1.006$ nm and $n_s a_s = 2.982 \times 10^{20}$ nm^2. We assume that the interface is constituted of only CTAB molecules in this range of $V(w)$. If, following Lang *et al.*,[10] we take $a_s = 0.45$ nm^2 (for CTAB): we obtain $n_s = 6.626 \times 10^{20}$, while the total number of CTAB molecules actually present in the system is 1.652×10^{21}. Thus, at this stage, only about 40% of all available CTAB molecules reside at the interface.

The deviation from linearity that is observed in region II suggests an increase in the total interfacial area [eqn. (3)]. So, in this region, an increase in the water content leads to a migration of the remaining CTAB molecules as well as the butanol molecules to the interface. The effective diameter should increase again when all surfactant and co-surfactant molecules occupy only the interface. However, it is unrealistic to interpret the measured correlation length as an effective diameter in region III, since well defined W/O droplets may not exist when the water content is so high.

Effect of Dilution with Oil

Fig. 6 shows a segment of the phase diagram of (CTAB + butanol)–octane–water at 25 °C. A movement from P_1 to P_4 in the phase diagram represents the dilution of a particular composition with oil while keeping constant the surfactant:water ratio. The four compositions studied were all confined to the L_2 (W/O microemulsion) region. Dilution with the external phase results in a nearly exponential increase in the effective diameter of the water droplets (Fig. 7). The increase in the droplet diameter is accompanied by an appreciable decrease in the polydispersity (a measure of the relative width of the droplet size distribution). Note that P_4

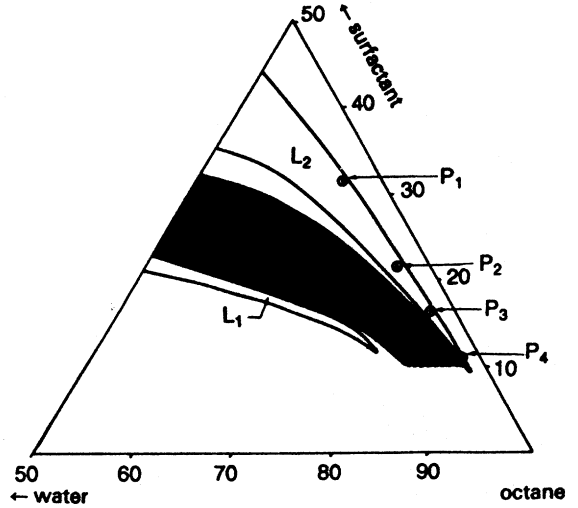

Fig. 6 Portion of the (CTAB + butanol)–octane–water phase diagram. Dilution with octane is represented by a shift along $P_1 \rightarrow P_2 \rightarrow P_3 \rightarrow P_4$ within the L_2 (water-in-oil microemulsion) region.

lies at the extreme tip of the L_2 region adjacent to an optically anisotropic (liquid crystalline?) phase. At P_4 the microstructure is that of large (*ca.* 40 nm), monodisperse W/O droplets: a precursor to the transition to a macroscopically ordered phase.

Effect of Changing Salt Concentration

We observed a gradual and linear decrease in D_h (Fig. 8) when the concentration of $Y(NO_3)_3$ was increased from 0.025 to 0.2 mol dm^{-3}, $f(w)$ being kept constant at *ca.* 10%. An increase in the salt concentration in the dispersed phase is expected to drive out the butanol molecules from the aqueous phase to the interface, leading to the observed decrease in the droplet diameter. A further increase in concentration would send the alcohol molecules out into the oil phase, which may explain the small increase in D_h above 0.2 mol dm^{-3}. The presence of an electrolyte in the dispersed phase would, in addition, reduce the repulsive force between the head groups of the surfactant molecules, leading to a more efficient packing and consequently a smaller radius of curvature.

The interdroplet interaction, however, is not strongly affected by a change in the $Y(NO_3)_3$ concentration between 0.025 and 0.3 mol dm^{-3}: the viscosity varies little in this range (Fig. 8). An increase in the salt concentration beyond 0.3 mol dm^{-3} presumably destroys the W/O microemulsion

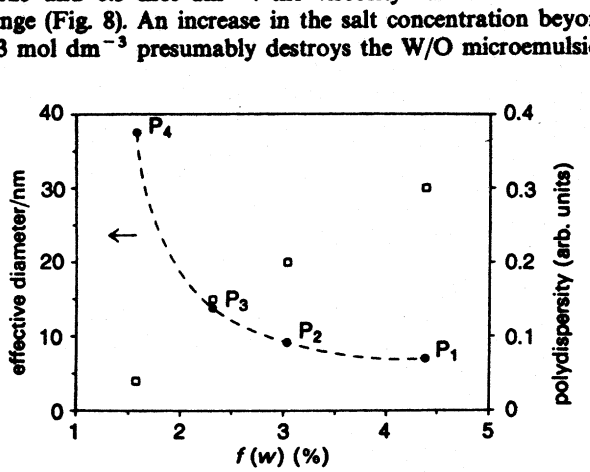

Fig. 7 Variation of the effective hydrodynamic diameter (●) due to dilution with oil for the (CTAB + butanol)–octane–water system. P_1 *etc.* refer to the compositions shown in Fig. 6. Empty squares represent the corresponding 'polydispersity'. (The dashed line is for visual guidance.)

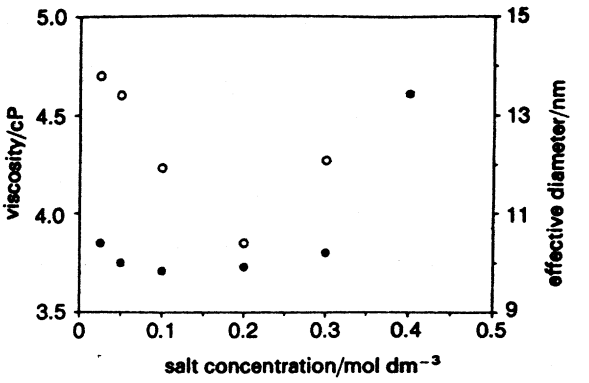

Fig. 8 Variation of the effective hydrodynamic diameter (○) and viscosity (●) with concentration of $Y(NO_3)_3$ for the (CTAB + butanol)–octane–$Y(NO_3)_3$ system with $f(w) \approx 10\%$ (fixed)

structure, resulting in a large increase in the viscosity and indeterminate values of the droplet size.

Optical Absorption Study of Cu^{II} Complex Formation

The dissolution of aqueous $Cu(NO_3)_2$ in CTAB–butanol–octane as W/O microemulsion leads to an interesting phenomenon. At low values of $f(w)$, less than 5%, the system shows an intense purple colour. This effect must be associated with the unique microenvironment of the Cu^{II} ions within the aqueous pools of the microemulsion since no such colouration is produced on simply adding CTAB to an aqueous solution of $Cu(NO_3)_2$.

For $f(w) \approx 5\%$, maximum optical absorption was found to occur at $\lambda_{max} = 535$ nm. We measured the absorbance, $\log(I_0/I)$, at $\lambda = \lambda_{max}$ for the CTAB–butanol–octane–$Cu(NO_3)_2$ system as a function of the aqueous phase fraction, $f(w)$. The concentration of the $Cu(NO_3)_2$ solution was kept fixed at 0.3 mol dm^{-3}. The reference cell contained only 0.3 mol dm^{-3} $Cu(NO_3)_2$, and at each stage of measurement, the same amount of $Cu(NO_3)_2$ solution was added to both the sample and reference cells. The rapid decrease in the absorbance with increasing $f(w)$ roughly coincides with the percolation threshold (Fig. 9). The microemulsion became visually colourless at $f(w) \approx 15\%$ and progressively acquired the light greenish-blue colour of hydrated Cu^{II} for higher $f(w)$.

The structure of copper halide complexes co-solubilized in cationic reverse micelles (CTAB–chloroform–Cu^{II} halide solution) has been studied by Sunamoto *et al.*[15] They found that at low water content ($w_0 \equiv [H_2O]/[CTAB] \leq 1$), the Cu^{2+} ions co-solubilized in the micelles form a polymeric

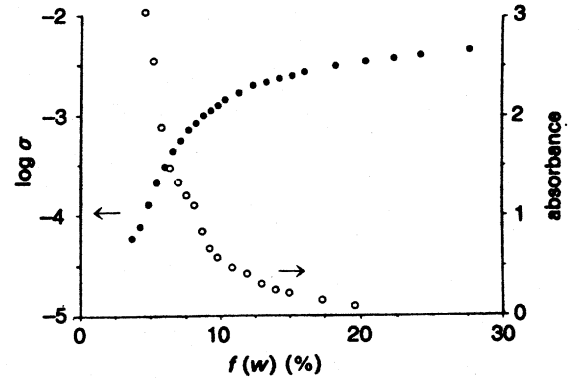

Fig. 9 Dependence of the absorbance at 535 nm (○) and the electrical conductivity [(●) in S cm^{-1}] on the aqueous fraction (wt.%) for the (CTAB + butanol)–octane–0.3 mol dm^{-3} $Cu(NO_3)_2$ system

chain with the halogen atoms acting as bridges between the Cu atoms. In this complex, the Cu atom is in a distorted tetrahedral configuration. With an increase in the water content ($w_0 \approx 2$–4), the polymeric Cu ions become monomeric, but still have a distorted tetrahedral configuration. Further increase in w_0 (>4) leads to the distorted octahedral structure characteristic of aqueous Cu^{II} salt solutions.

The system studied by Sunamoto *et al.* differs from ours in two important respects. They injected a fixed quantity of CuX_2 into the CTAB–chloroform solution initially and studied the system while adding water: thus $[Cu^{2+}]$ kept decreasing progressively. In contrast, we observed our system spectroscopically while adding an aqueous solution of Cu^{2+}, thereby keeping $[Cu^{2+}]$ fixed within the microemulsion droplet. Secondly, in the earlier system, the aqueous component is partitioned into the dispersed and continuous (chloroform) phases and gets pulled into the micellar core with increasing w_0. No such partitioning is expected in the present case. Since $[Cu^{2+}]$ remained strictly constant, the changes in the Cu ion coordination observed by us can be ascribed to changes in $f(w)$ and droplet size. Below $f(w) \approx 8\%$ (corresponding to $w_0 \leq 9$), Cu^{2+} exists as the complex $[CuBr_3]^- \cdot 2H_2O$ ion recognized by its characteristic intense purple colour. This complex is normally formed[16] when $CuBr_2$ is dissolved in concentrated HBr. With increasing $f(w)$ (and droplet size) the complex breaks down and the Cu ion assumes the hydrated form: $[Cu(H_2O)_6]^{2+}$, which has a light blue colour.

Conclusions

Conductivity, viscosity and light scattering data provide definite indications about the microscopic structure of the (CTAB + butanol)–octane–aqueous salt system. Changes in properties were studied along particular directions in the phase diagram but the conclusions should apply qualitatively all over the isotropic single-phase region. We emphasize that the quantity D_h obtained from QELS is an aqueous phase correlation length and can be interpreted as an 'effective diameter' only in low-water-content systems. For more complicated bicontinuous structures, it can be loosely understood as an average radius of curvature of the interface.

When the aqueous content is below the percolation threshold, $f_p \approx 12\%$, the isolated aqueous droplets interact relatively weakly. With increasing water content, the correlation length of the aqueous phase increases linearly (from 7 to 18 nm). Even above the percolation threshold, the aqueous droplets appear to retain their identity but probably form either weakly bound clusters or a bicontinuous phase. The surfactant aggregation number changes in this regime, as surfactant molecules migrate from the continuous phase to the interface. The consequent decrease in the correlation length continues till this migration is complete.

When Cu ions are present in the water phase, they form a complex with the Br^- counter-ions of CTAB, producing a vivid purple colour. The complexation occurs only in the extremely dilute microemulsion limit and the complex breaks down with an increase in the size of the aqueous droplets. This is therefore a 'size-effect'.

Microemulsions have found application in the synthesis of nanocrystalline metals[17] and metal oxides.[18] Soluble metal salts are encapsulated in the core of a W/O microemulsion and precipitated within them. The (CTAB + butanol)–octane system can solubilize, below the percolation threshold, a substantial amount of salt solution as well defined, isolated inverse micelles. This property has been utilized in the synthesis of microhomogeneous, ultrafine particles of superconducting $YBa_2Cu_3O_{7-\delta}$.[19,20]

The study was supported by a grant from the Defence Advanced Research Project Agency. It is a pleasure to thank Professor M. S. Multani for his advice and encouragement.

References

1 L. E. Scriven, *Nature (London)*, 1976, **263**, 123.
2 *Microemulsions: Theory and Practice*, ed. L. M. Prince, Academic, New York, 1977.
3 *Microemulsions*, ed. I. D. Robb, Plenum, New York, 1982.
4 *Reverse Micelles*, ed. P. L. Luisi and B. E. Straub, Plenum, New York, 1984.
5 B. Lindman, N. Kamenka, T-M. Kathopoulis, B. Brun and P-G. Nilsson, *J. Phys. Chem.*, 1980, **84**, 2485.
6 M. Dvolaitzky, M. Guyot, M. Lagues, J-P. Lepesant, R. Ober, C. Sauterey and C. Taupin, *J. Chem. Phys.*, 1978, **69**, 3279.
7 M. Zulauf and H-F. Eicke, *J. Phys. Chem.*, 1979, **83**, 480.
8 M. J. Hou, M. Kim and D. O. Shah, *J. Colloid Interface Sci.*, 1988, **123**, 398.
9 A. M. A. Da Costa, C. F. G. C. Geraldes and J. J. C. Teixeira-Dias, *J. Colloid Interface Sci.*, 1982, **86**, 254.
10 J. Lang, G. Mascolo, R. Zana and P. L. Luisi, *J. Phys. Chem.*, 1990, **94**, 3069.
11 C. Gamboa and L. Sepulvada, *J. Colloid Interface Sci.*, 1986, **113**, 566.
12 Th. F. Tadros, in *Surfactants in Solutions*, ed. K. L. Mittal and B. Lindman, Plenum, New York, 1984, vol. 3, p. 1522.
13 S. A. Safran, G. S. Grest and A. L. R. Bug, in *Microemulsion Systems*, ed. H. L. Rosano and M. Clausse, Marcel Dekker, New York, 1987, p. 235.
14 D. F. Evans, D. J. Mitchell and B. W. Ninham, *J. Phys. Chem.*, 1986, **90**, 2817.
15 J. Sunamoto, H. Kondo, T. Hamada, S. Yamamoto, Y. Matsuda and Y. Murakami, *Inorg. Chem.*, 1980, **19**, 3668.
16 M. C. Sneed, J. L. Maynard and R. C. Brasted, *Comprehensive Inorganic Chemistry*, van Nostrand, New York, 1954, vol. 2, p. 80.
17 M. Boutonnet, J. Kizling, P. Stenius and G. Maire, *Colloid Surf.*, 1982, **5**, 209.
18 P. Ayyub, M. Multani, M. Barma, V. R. Palkar and R. Vijayaraghavan, *J. Phys. C*, 1988, **21**, 2229.
19 P. Ayyub, A. N. Maitra and D. O. Shah, *Physica C*, 1990, **168**, 571.
20 P. Ayyub and M. S. Multani, *Mater. Lett.*, 1991, **10**, 431.

Paper 3/02562D; *Received* 5th *May*, 1993